LARGE AMPLITUDE WAVE-TRAINS OF COSMIC-RAY INTENSITY

H. MAVROMICHALAKI
Nuclear Physics Laboratory, University of Athens, Greece

(Received 16 November, 1979)

Abstract. The large amplitude wave-trains of cosmic-ray intensity observed during June, July and August, 1973, were analysed. These events exhibit the same characteristics as the event of May, 1973. During these days the phase of the enhanced diurnal anisotropy is shifted to a point earlier than either the corotation direction or the anti-garden-hose direction. For this analysis we used data from high- and middle-latitude neutron monitors and from the satellites HEOS-2, IMP-7 and IMP-8. The diurnal variation of these days is well understood in terms of a radially outward convective vector and a field-aligned inward diffusive vector yielding a diurnal anisotropy vector along about 1600 h in space.

1. Introduction

The diurnal anisotropy of cosmic-ray intensity has recently been explained in terms of a convective and diffusive mechanism. It is interesting, therefore, to understand, via this mechanism, the large variation observed in phases and amplitudes on a day-to-day basis. Periods of unusually large amplitude often occur in trains of several days. The amplitudes of these interesting variations cannot be explained by the corotation effect which usually predicts values of 0.4%. Moreover, the maximum intensity of diurnal anisotropy has not appeared in the direction of 1800 h, which is the nominal corotation phase (McCracken and Rao, 1965; Rao, 1972).

A lot of research has been undertaken to find a possible origin for these 'large amplitude wave-trains' of cosmic-ray neutron intensity. Hashim and Thambyahpillai (1969) and Rao *et al.* (1972) have shown that the enhanced diurnal variation of large amplitude events exhibits a maximum intensity in space around the anti-garden-hose direction (2000 h) and a minimum intensity around the garden-hose direction (900 h). Kane (1970) and Bussoletti (1973) have noticed that large reinforcements often come from the corotation direction. In all these cases the observed diurnal anisotropy is well understood in terms of a convective–diffusive mechanism (Forman and Gleeson, 1975). Recently it has been shown (Mavromichalaki, 1979) that the enhanced diurnal variation observed over the period of 22 May to 4 June, 1973, was caused by a source around 1600 h or by a sink at about 400 h. It was pointed out that this diurnal variation is caused by the superposition of convection and field-aligned diffusion due to an enhanced density gradient of $\sim 8\%\ \mathrm{AU}^{-1}$.

In the present work a systematic and detailed analysis of another three large amplitude events has been performed. The events studied exhibit the same characteristics

Astrophysics and Space Science **71** (1980) 101–110. 0004–640X/80/0711–0101$01.50

as those of the event mentioned above. Similar results have been obtained, namely the phase of this diurnal variation in space is shifted to an earlier point (1600 h), which is satisfactorily explained by the convective–diffusive mechanism. Thus, a new class of large amplitude wave-trains of cosmic-ray intensity has appeared. The phase of these events is shifted to a point earlier than either the anti-garden-hose direction or the corotation direction. The explanation by the convective–diffusive mechanism supports this model in a study of enhanced diurnal variation.

In this paper the sequences of the large amplitude events observed over the periods 11–18 June, 11–20 July and 9–18 August, 1973, have been selected for analysis.

2. Data Analysis

The characteristics of cosmic-ray diurnal anisotropy during these events have been determined from the data analysis of a few high- and middle-latitude neutron monitoring stations. These stations are properly distributed in longitude and have narrow asymptotic cones of acceptance. To correct the cosmic-ray intensity from the north–south anisotropy, data from the two 'polar' stations, Alert and McMurdo, were also used. All the stations from which data have been used in the present work are listed in Table I.

TABLE I

Neutron monitoring stations from which data have been used in the present analysis

Station (NM-64)	Symbol	Geographic coordinates		Threshold rigidity (GV)	Mean asymptotic coordinates	
		Latitude (deg.)	Longitude (deg.)		Latitude (deg.)	Longitude (deg.)
Sanae	SA	−70.30	357.7	1.06	−21	19
Leeds	LE	53.8	358.5	2.20	4	52
Utrecht	UT }	52.1	5.1	2.76	−2	62
Kiel	KI }	54.3	10.1	2.29	3	64
Oulu	OU }	65.0	25.4	0.81	30	63
Kerguelen	KE	−49.4	70.2	1.19	−26	87
Novosibirsk	NO	54.8	83.0	2.91	10	130
Magadan	MA	60.1	151.0	2.10	12	191
Inuvik	IN	68.4	226.3	0.18	47	233
Calgary	CA	51.1	245.9	1.09	28	269
Climax	CL	39.4	253.8	3.03	26	296
Deep River	DR	46.1	282.5	1.02	27	319
Swarthmore	SW }	39.9	284.6	1.92	−10	331
Durham	DU }	43.1	289.2	1.41	25	332
Goose Bay	GB }	53.3	299.6	0.52	35	339
Alert	AL	82.5	297.7	< 0.05	77	331
McMurdo	MC	−77.9	166.6	< 0.05	−74	261

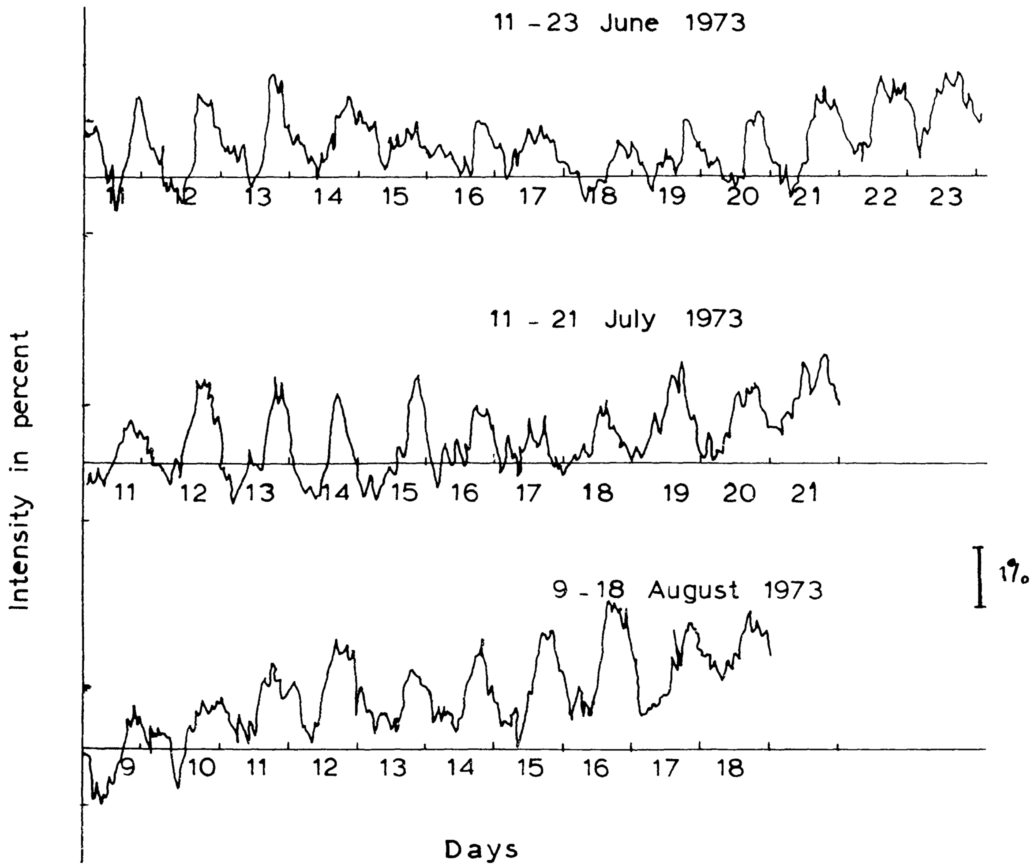

Fig. 1. Intensity–time diagrams of the three events, as observed at the Deep River neutron monitoring station.

The mean intensity for three days prior to the commencement of each enhanced diurnal wave-train was used for normalization of each station. The time-dependence of the percentage departures in intensity from this level, as observed at the Deep River neutron monitoring station, is shown in Figure 1.

From the hourly intensity of each station we subtracted the mean intensity at Alert and McMurdo. Combining the intensities from all the stations at each azimuthal direction relative to the Sun–Earth line in space, three-dimensional space–time maps of cosmic-ray intensity in space were constructed (Mercer and Wilson, 1968; Hashim and Thambyahpillai, 1969; Rao *et al.*, 1972; Mavromichalaki, 1979). These maps define the cosmic-ray intensity of the equatorial diurnal anisotropy as a function of direction at any given time and are ideally suited to study the characteristics of anisotropy. Such maps are plotted on an hour-to-hour and day-to-day basis, but space limitations prevent us from presenting them here (see Mavromichalaki, 1979). The amplitude and phase of the equatorial diurnal anisotropy for each day were estimated by the method developed by Bussoletti *et al.* (1972). The data are corrected for geomagnetic bending.

The interplanetary field parameters for each of these days were obtained from the measurements of the HEOS-2, IMP-7 and IMP-8 satellites for comparison with the diurnal anisotropy vectors.

3. Experimental Results

The events analysed here seem to be a repetition of the large amplitude event which occurred from 22 May to 4 June, 1973, with the difference that the amplitude of this diurnal anisotropy is smaller. In any case, the half-peak amplitude of the anisotropy detected at ground level for those periods is equal to or greater than 0.80%, assuming that the diurnal variation of those days is 'enhanced'. These time periods are not connected with Forbush decreases and the general conditions in interplanetary space are quiet.

It is very useful to underline here the similarities between the morphology of these wave-trains and that of May, 1973, previously analysed (Mavromichalaki, 1979). The study of the space–time maps of these events has shown that the pattern of the corotative component of the diurnal variation is far from constant. In fact the amplitude of the diurnal anisotropy in interplanetary space is greater than the

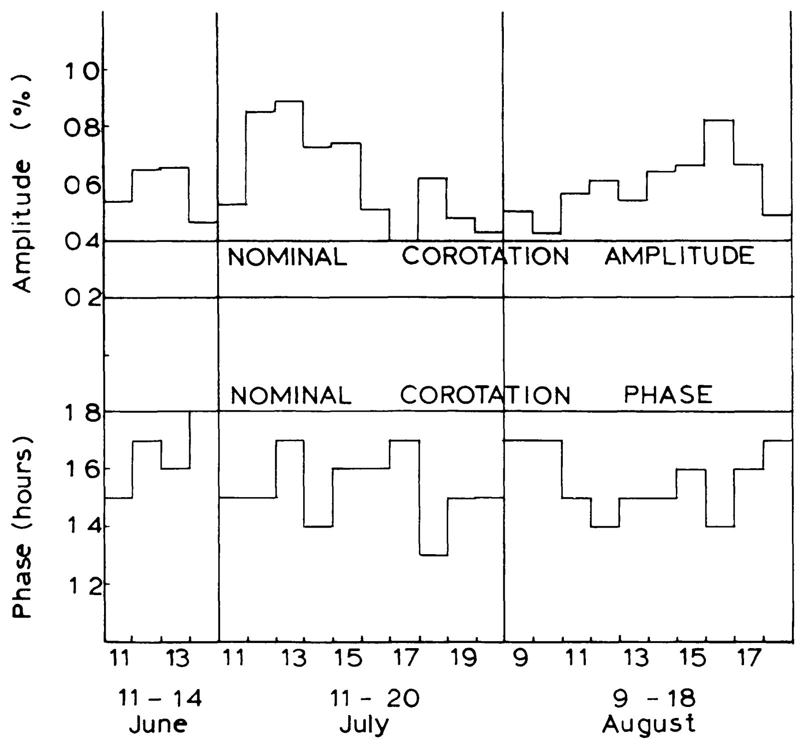

Fig. 2. The amplitude and phase of the diurnal anisotropy in space on each day of the three large amplitude events from a number of neutron monitoring stations.

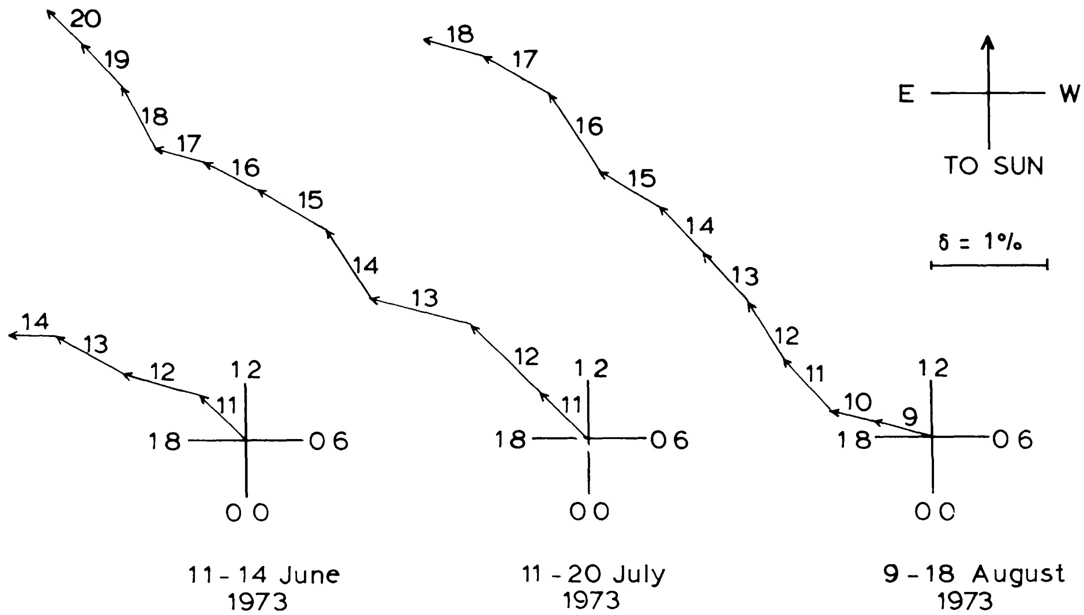

Fig. 3. The diurnal anisotropy vectors for each day plotted end to end for each of the three events.

nominal corotation amplitude (0.4%) and the direction of maximum intensity is shifted to an earlier time than the 1800 h direction predicted by the corotation theory. The diurnal anisotropy is observed to show a maximum intensity at approximately 1600 h the direction during the entire period of these large amplitude events. The diurnal anisotropy maximum, and the time of maximum for each day, are shown in Figure 2. The mean observed phase of the diurnal anisotropy in space for the events of June, July, and August, 1973, is the direction of 1600, 1500 and 1600 h, respectively. The estimated diurnal anisotropy vectors for each day, plotted end to end for each of the three events, are shown in Figure 3.

Previous analyses of such events had shown that the enhanced daily variation is due to a decrease of cosmic-ray intensity in the garden-hose direction (Mathews *et al.*, 1969; Hashim and Thambyahpillai, 1969; Ananth *et al.*, 1971) or to an increase of cosmic-ray intensity in the anti-garden-hose direction (Rao *et al.*, 1972). Also, the anisotropy maximum frequently presents an increased intensity along the corotational direction (Kane, 1970; Bussoletti, 1973). As noticed recently (Mavromichalaki, 1979), the enhanced diurnal variation can be due to an enhanced intensity in the direction of 1600 h and a depressed intensity in the direction of 400 h. During these events an enhanced cosmic-ray intensity is observed in a broad cone of directions around 60° E of the Sun–Earth line. It is noticed that the intensity in the garden-hose and anti-garden-hose directions of the interplanetary magnetic field is almost unaffected.

4. Field-Aligned Diffusion During Days of Enhanced Diurnal Variation

In order to explain the observed phase shift of the diurnal anisotropy to earlier points and to establish the field-aligned nature of the diffusive flow during these events, the observed cosmic-ray diurnal anisotropy vector δ was resolved into two components

$$\delta = \delta_c + \delta_d, \tag{1}$$

where δ_c is the convective vector and δ_d the diffusive vector. The magnitude of the convective vector was calculated by the expression (Rao *et al.*, 1972)

$$\delta_c = 3C\frac{V_p}{v}, \tag{2}$$

where C is the Compton–Getting factor (which is 1.5 for neutron-monitor energies), V_p the solar wind velocity and v the particle velocity. The diffusive anisotropy vectors for each day were calculated with the help of relation (1). These vectors were compared with the ecliptic component of the interplanetary magnetic field.

The solar wind data were obtained from IMP-7 and IMP-8 satellite measurements and the interplanetary magnetic field data from magnetometers aboard the HEOS-2 satellite. The observed diurnal anisotropy vector, the convective vector, the diffusive vector and the interplanetary magnetic field vector (ecliptic component) for each day of the three large amplitude events are given in the Tables II, III and IV, respectively. Unfortunately, no data are available of the interplanetary parameters for all days during the enhanced diurnal variation. The diffusive anisotropy vector for the three events, day-to-day, is shown in Figure 4. The ecliptic component of the interplanetary magnetic field, B_{xy}, plotted alongside the diffusive vector for each day, is also shown in the same figure. Note the good agreement between the field azimuth and the direction of the diffusive vector throughout the duration of the events, except 14 July and 16 August where there is a small deviation from the anti-garden-hose

TABLE II

Diurnal anisotropy vector, convective vector, diffusive vector and interplanetary magnetic field vector (ecliptic component) for the event of June, 1973

June, 1973	Diurnal anisotropy vector		Convective vector	Diffusive vector		Magnetic field vector	
	Amplitude (%)	Phase (deg.)	Amplitude (%)	Amplitude (%)	Phase (deg.)	Amplitude (γ)	Phase (deg.)
11	0.54	225	0.81	0.57	319	7.26	340
12	0.65	255	0.93	0.98	321	5.43	325
13	0.67	240	1.02	0.90	320	5.38	340
14	0.47	270	0.92	1.03	333	4.22	342

TABLE III

Diurnal anisotropy vector, convective vector, diffusive vector and interplanetary magnetic field vector (ecliptic component) for the event of July, 1973

July, 1973	Diurnal anisotropy vector		Convective vector	Diffusive vector		Magnetic field vector	
	Amplitude (%)	Phase (deg.)	Amplitude (%)	Amplitude (%)	Phase (deg.)	Amplitude (γ)	Phase (deg.)
11	0.53	225	0.55	0.41	296	4.98	316
12	0.85	225	0.53	0.60	263	4.36	301
13	0.89	255	0.58	0.66	293	4.47	297
14	0.73	210	0.66	0.37	275	7.12	338
15	0.74	240	0.94	0.85	312	8.26	322
16	0.51	240	0.86	0.75	324	3.37	290
17	0.39	255	0.69	0.70	327	3.61	346
18	0.62	195					
19	0.48	225					
20	0.43	225					

direction. In any case, the field-aligned nature of the diffusion vector on a day-to-day basis during these events is confirmed. During these days the magnetic field was continuously directed away from the Sun, therefore it is not possible to have results about the days which are influenced by magnetic sector boundaries or when the magnetic field is directed towards the Sun.

TABLE IV

Diurnal anisotropy vector, convective vector, diffusive vector and interplanetary magnetic field vector (ecliptic component) for the event of August, 1973

August, 1973	Diurnal anisotropy vector		Convective vector	Diffusive vector		Magnetic field vector	
	Amplitude (%)	Phase (deg.)	Amplitude (%)	Amplitude (%)	Phase (deg.)	Amplitude (γ)	Phase (deg.)
9	0.50	255	0.51	0.62	308	5.13	323
10	0.42	255	0.49	0.56	313	2.68	314
11	0.56	225	0.47	0.40	282	2.60	294
12	0.61	210	0.45	0.31	255	4.10	281
13	0.54	225				8.42	323
14	0.64	225				5.53	339
15	0.66	240				4.69	331
16	0.82	210	0.53	0.45	246	3.36	325
17	0.67	240	0.48	0.60	284	2.71	313
18	0.49	255	0.46	0.58	305	2.51	290

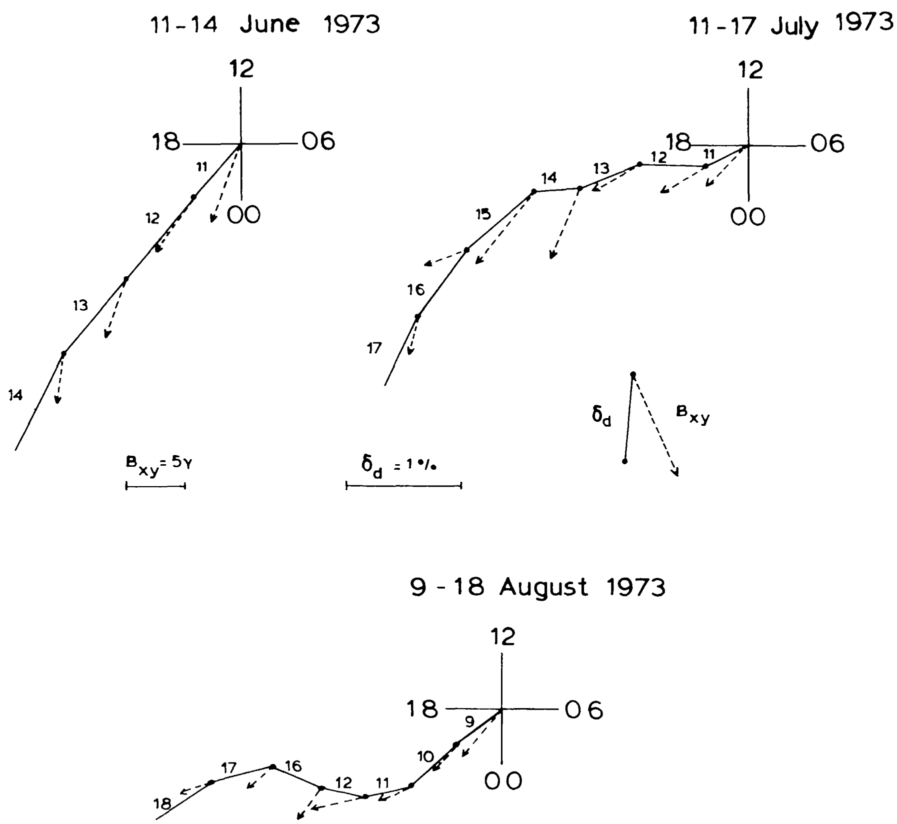

Fig. 4. The ecliptic component of the magnetic field vector for each day plotted alongside the diffusive vector for each of the three enhanced diurnal variation events.

5. Discussion and Conclusions

The convective–diffusive mechanism, as applied to cosmic-rays at neutron monitoring energies in the solar system, involves diffusion which is essentially field-aligned (Jokipii, 1971). This mechanism is appropriate in this energy range when perpendicular diffusion is very small in comparison with parallel diffusion. Moreover, Hashim and Bercovitch (1972) and Rao *et al.* (1972) have shown that the enhanced diurnal variation of cosmic rays can also be explained in terms of this mechanism.

Later, Kane (1974) and Ananth *et al.* (1974) showed that on a day-to-day basis the diffusion vector deviates from the direction of the interplanetary magnetic field in the ecliptic plane by more than 30° on about 35% of the quiet days. They have attempted to study the characteristics of these days, but have reached no conclusions. Owens and Kash (1976) have noticed that during the days which are influenced by interplanetary magnetic sector passages the diffusion vectors are not well field-aligned.

In this work we have given some new information on the study of large amplitude events in order to develop a suitable realistic theoretical model which could explain the diurnal anisotropy for all days, and the following conclusions are derived from the above analysis:

(a) The observed enhanced diurnal variation can be well understood in terms of an outward convection and a field-aligned diffusion yielding a diurnal anisotropy vector along about 1600 h in space.

(b) The diffusion follows in time the anti-garden-hose direction of the magnetic field. Moreover, it has been shown (Mavromichalaki, 1979) that diffusion maintains an anti-garden-hose direction irrespective of the direction of the magnetic field with respect to the Sun.

(c) According to the convective–diffusive mechanism (Kane, 1974) the ratio $K_\perp/K_\parallel$ of the perpendicular to parallel diffusion coefficient with respect to the ecliptic magnetic field as well as the transverse diffusion coefficient are negligible in a field-aligned diffusion vector. The anisotropy is then satisfactorily explained in terms of convection and diffusion. Ananth *et al.* (1974) have shown that, on average, the ratio $K_\perp/K_\parallel$ is $\leqslant 0.05$ for field-aligned days and ~ 1.0 for non-field-aligned days. During these events $K_\perp/K_\parallel$ was 0.24 for June, 0.30 for July and 0.36 for August. This means that the transverse gradients are negligible and the diffusion vector is assumed as field-aligned.

(d) During these events the radial density gradients in the ecliptic plane, which correspond to the average diffusion vectors, are $9\%\ \mathrm{AU}^{-1}$ for June, $6\%\ \mathrm{AU}^{-1}$ for July and $4.5\%\ \mathrm{AU}^{-1}$ for August, according to the method of Rao *et al.* (1972). In other words, large cosmic-ray gradients seem to exist especially during the event of June. The enhanced gradients during these events are caused by an increase of cosmic-ray intensity along the direction of 1600 h or by a decrease along the direction of 400 h.

(e) The phase shift of the enhanced diurnal anisotropy to an earlier point is explained by the convective–diffusive mechanism either as an enhancement in the convective vector or as a decrease in the diffusive vector (Agrawal and Singh, 1975). Recently Kumar *et al.* (1979) noticed that the diurnal time of maximum had shifted very significantly to an earlier point since 1971, and onwards on geomagnetic quiet days.

The analysis of these events, and the previously analysed event of May 1973, led us to the conclusion that these events constitute a new class of large amplitude wave-trains where the enhanced diurnal variation may be caused by a source at about 1600 h or by a sink at about 400 h. This diurnal anisotropy is correlated with neither the garden-hose nor the corotation directions. Thus, the problem of the origin of the large amplitude events is still under investigation. It may be that other sources or sinks of cosmic-ray intensity with different mechanisms exist. Further efforts may be needed to identify and characterize such sources or sinks of cosmic-ray intensity which can explain all the large amplitude wave-trains. In any case, the simple picture of outward convection and field-aligned diffusion also describes this diurnal anisotropy.

Acknowledgements

Thanks are due to the Director of WDC-A for the data of neutron monitors, to the experimental groups which contributed these data, and to Dr P. C. Hedgecock and to Dr H. Rosenbauer for magnetic field data and solar wind data. Many thanks are also due to Dr T. Thambyahpillai for his valuable comments and discussions.

References

Agrawal, S. P. and Singh, R. L.: 1975, *14th Int. Cosmic-Ray Conf.* (*München*) **4**, 1193.
Ananth, A. G., Agrawal, S. P. and Rao, U. R.: 1971, *12th Int. Cosmic Ray Conf.* (*Hobart*) **2**, 651.
Ananth, A. G., Agrawal, S. P. and Rao, U. R.: 1974, *Pramana*, **3**, 74.
Bussoletti, E.: 1973, *Eldo-Cesles/Esro-Cers Scient. Tech. Rev.* **5**, 285.
Bussoletti, E., Iucci, N. and Villoresi, G.: 1972, *Nuovo Cimento* **10B**, 43.
Forman, M. A. and Gleeson, L. J.: 1975, *Astrophys. Space Sci.* **32**, 77.
Hashim, A. and Bercovitch, M.: 1972, *Planet. Space Sci.* **20**, 791.
Hashim, A. and Thambyahpillai, T.: 1969, *Planet. Space Sci.* **17**, 1879.
Jokipii, J. R.: 1971, *Rev. Geophys. Space Phys.* **9**, 27.
Kane, R. P.: 1970, *J. Geophys. Res.* **75**, 4350.
Kane, R. P.: 1974, *J. Geophys. Res.* **79**, 1321.
Kumar, S., Vadava, R. S. and Agrawal, S. P.: 1979, *16th Int. Cosmic-Ray Conf.* (*Kyoto*) **4**, 86.
Mathews, T., Venkatesan, D. and Wilson, B. G.: 1969, *J. Geophys. Res.* **74**, 1218.
Mavromichalaki, H.: 1979, *Astrophys. Space Sci.* **60**, 59.
McCracken, K. G. and Rao, U. R.: 1965, *Cosmic-Ray Conf.* (*London*) **1**, 213.
Mercer, J. B. and Wilson, B. G.: 1968, *Can. J. Phys.* **46**, S849.
Owens, A. J. and Kash, M. M.: 1976, *J. Geophys. Res.* **81**, 3471.
Rao, U. R.: 1972, *Space Sci. Rev.* **12**, 719.
Rao, U. R., Ananth, A. G. and Agrawal, S. P.: 1972, *Planet. Space Sci.* **20**, 1799.